

Structural phase transition in vanadium at high pressure and high temperature: Influence of nonhydrostatic conditions

Zs. Jenei,^{1,2} H. P. Liermann,^{3,4} H. Cynn,¹ J.-H. P. Klepeis,¹ B. J. Baer,¹ and W. J. Evans¹

¹*Condensed Matter & Materials Division, Physical & Life Sciences Directorate, Lawrence Livermore National Laboratory, Livermore, California 94551, USA*

²*Department of Physics, Stockholm University, S-106 91 Stockholm, Sweden*

³*High-Pressure Collaboration Access Team (HPCAT), Geophysical Laboratory, Carnegie Institution of Washington, c/o Advance Photon Source, Argonne National Lab, Argonne, Illinois 60439, USA*

⁴*Hamburger Synchrotronstrahlungslabor (HASYLAB), Deutsches Elektronen-Synchrotron (DESY), Petra III, P02, Notkestrasse 85, D-22607 Hamburg, Germany*

(Received 4 May 2009; revised manuscript received 31 August 2010; published 7 February 2011)

Vanadium has been reported to undergo phase transition upon compression from body-centered cubic (bcc) to rhombohedral structure around 62 GPa. In this paper we confirm the bcc to rhombohedral phase transition at 61.5 GPa under quasihydrostatic compression in the Ne pressure medium. Under the nonhydrostatic condition we find the phase transition occurring at 30 GPa at ambient temperature and 37 GPa at 425 K. We find the transition under the hydrostatic condition is hindered and it can occur at much lower pressure under the nonhydrostatic condition.

DOI: [10.1103/PhysRevB.83.054101](https://doi.org/10.1103/PhysRevB.83.054101)

PACS number(s): 62.50.-p, 64.70.-p, 61.50.Ks

I. INTRODUCTION

Vanadium is a transition metal that has been the subject of recent theoretical and experimental studies. Early theoretical studies of the structural phase stability, based on a simple model, predicted most of the trends in the transition metals regarding their structure under ambient and high-pressure conditions.¹ The prediction of a very stable body-centered cubic (bcc) structure for group 5 transition metals was confirmed in the case of Ta, up to ~ 200 GPa.² However, in the case of vanadium this prediction of a very stable bcc structure is not consistent with the experimental results and modern theoretical calculations.

In a theoretical study of the superconducting transition temperature behavior under high pressure conditions, Suzuki and Otani performed first-principles calculations of the lattice dynamics of vanadium in the pressure range of up to 150 GPa.³ They found that the transverse acoustic phonon mode TA [$\xi 00$] around $\xi = 1/4$ shows a dramatic softening under pressure and becomes imaginary above 130 GPa, indicating the possibility of a structural phase transition. Later, Landa *et al.* performed total energy calculations for the trigonal shear elastic constant (C_{44}) of vanadium in the bcc phase.⁴ Their results identified a mechanical instability in C_{44} around 200 GPa, preceded by a change in the slope of its pressure dependence beginning at ~ 60 GPa. The authors attribute the instability in the trigonal shear elastic constant to an intraband nesting feature of the Fermi surface.

Later Ding *et al.* performed experimental studies, confirming that indeed vanadium undergoes a pressure-induced phase transition from the bcc to a rhombohedral structure at 69 GPa.⁵ Further first-principles calculations confirmed the experimental identified rhombohedral phase in vanadium.^{6,7} Furthermore, Lee *et al.* found two different rhombohedral phases in their studies' β , γ phases that differ from each other only in the angle between the rhombohedral basis vectors. The stability range of these two rhombohedral phases are followed by a transition back to the bcc structure above

280 GPa pressure, which is predicted to remain the energetically stable structure up to at least 400 GPa according to Luo *et al.*⁸ The most recent theoretical study of vanadium phase stability indicates the transition to the first rhombohedral phase at 60 GPa and the transition to the high-pressure bcc phase at 310 GPa.⁹

It is interesting to note that Ding *et al.* found that under nonhydrostatic conditions the phase transition from the bcc to rhombohedral structure occurred at a higher pressure of 69 GPa, in contrast to the transition pressure of 63 GPa under quasihydrostatic conditions. These results are at odds with the typical expectation that nonhydrostatic conditions lower the transition pressure compared to hydrostatic and quasihydrostatic conditions.^{10–12} This unusual behavior of the reported phase transition prompted our interest in further studies of the transition. In the following we present our findings using both nonhydrostatic and quasihydrostatic pressure transmitting media.

II. EXPERIMENT

For our high-pressure studies of vanadium, we used a membrane diamond-anvil cell (mDAC) with 0.2-mm flat and 0.1/0.3-mm beveled diamond anvils for moderate and high-pressure ranges, respectively. We used 0.25-mm thick Re gaskets, preindented to up to 25 GPa, corresponding to gasket thickness of 21–24 μm . Either a 120 μm (moderate pressure) and 60 μm (high pressure) hole was electric discharge machine (EDM) drilled in the center of the indented area to form the sample chamber. The source for the sample was Alfa Aesar's vanadium powder, -325 mesh, with a purity of 99.5%. For quasihydrostatic experiments small, 5–10- μm diameter vanadium grains were loaded together with a small Pt particle for a pressure marker. The pressure transmitting media (argon, neon, helium) was loaded in a 30,000-psi high-pressure gas loader at 0.165 GPa, with the initial pressure manually increased to 2–3 GPa with the screws in the loading chamber. For nonhydrostatic studies

the sample chamber was packed with V powder and a few Pt particles ($<2 \mu\text{m}$ size) were added to serve as a pressure marker. The choice for the pressure marker of Pt was motivated by two reasons: (1) It has minimal overlapping lines with the diffraction pattern of the sample, and (2) a well-calibrated high pressure and temperature equation of state (EOS). Even with these benefits, we were very careful to use in our analysis clean diffraction patterns, containing diffraction only from the sample. To heat the sample we chose a simple method of wrapping a commercial heating coil (Tempco, Inc.) around the mDAC and insulating it from ambient heat sinks using several layers of aluminum foil. This simple approach was possible since our target temperatures were less than 200°C . Angle dispersive x-ray diffraction (XRD) experiments were carried out at the High-Pressure Collaboration Access Team (HPCAT) at the Advanced Photon Source at Argonne National Laboratory, at Sector 16. Diffraction patterns were collected over the course of several different experimental runs using monochromatic x-ray beams typically of 25 or 30 keV. The diffraction patterns were collected with a MAR345 image plate with typical exposure times varying between 30–120 s. The two-dimensional (2D) images collected were integrated using Fit2D¹³ to obtain an intensity curve of the diffraction peaks as a function of the 2θ angle, which were analyzed to obtain the cell parameters using the XRDA¹⁴ and JADE software packages.

III. RESULTS AND DISCUSSION

Our initial study was carried out on a sample loaded without a pressure medium and compressed to pressures well beyond the phase transition pressure ($>15 \text{ GPa}$). During the transition from the bcc to the rhombohedral structure, it can be seen in the integrated pattern that the bcc 110 and 211 peaks split into two and three peaks, respectively. Initially the new rhombohedral peaks are very close to each other and cannot be resolved in the integrated 2θ -intensity plot. However, in the 2D image of the Debye-Scherrer rings, distinct lines could be seen at different positions. What is easily measurable on the integrated pattern is the width of individual diffraction peaks and a broadening of the previously mentioned two peaks can be observed. These changes are easily identified since the 200 peak from the bcc does not split through the transition, and remains very sharp. In Fig. 1 we present a few representative integrated 2θ -intensity diffraction patterns from the nonhydrostatic sample, the broadening of the 110 and 211 peaks is evident and used to identify the transition and becomes more pronounced with the increasing pressure. To within the experimental accuracy, we do not observe an abrupt splitting of the diffraction peaks, but instead a continuous and increasing separation. This, in the pressure range relevant to the transition, can be seen in Fig. 2 where we show the width of the 110 peak as a function of the pressure. At 82 GPa under nonhydrostatic compression the split of the 110 bcc peak into the 110 and 100 rhombohedral peaks is clearly visible in the 2D diffraction image shown in Fig. 3. While the individual peaks of the split 211 bcc peak are not distinguishable, the strong broadening of the ring can be observed. Our experiments at room temperature for nonhydrostatic compression identify a transition pressure

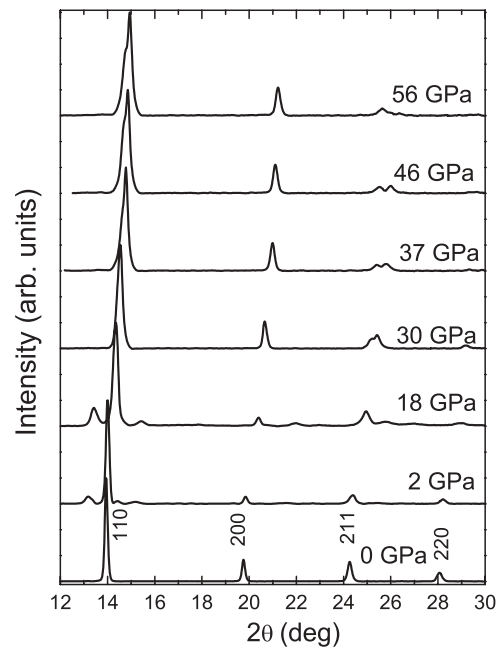


FIG. 1. Integrated XRD patterns of vanadium showing broadening of 110 and 211 peaks across the bcc-rhombohedral transition as compressed without pressure media under nonhydrostatic conditions ($\lambda = 0.51822 \text{ \AA}$).

of 30 GPa, which is much lower than previously reported by Ding *et al.* Our data show unambiguously that the phase transition occurs at this lower pressure both from the peak broadening and the diffraction pattern hkl indexing, which fits the rhombohedral structure very well. To confirm this lower transition pressure of 30 GPa and determine the temperature dependence, we performed nonhydrostatic compression experiments on several different samples at ambient and at higher temperature as well. Raising the sample temperature to 425 K yielded similar results: During compression of the sample from 20 to 75 GPa we observe changes in the diffraction patterns

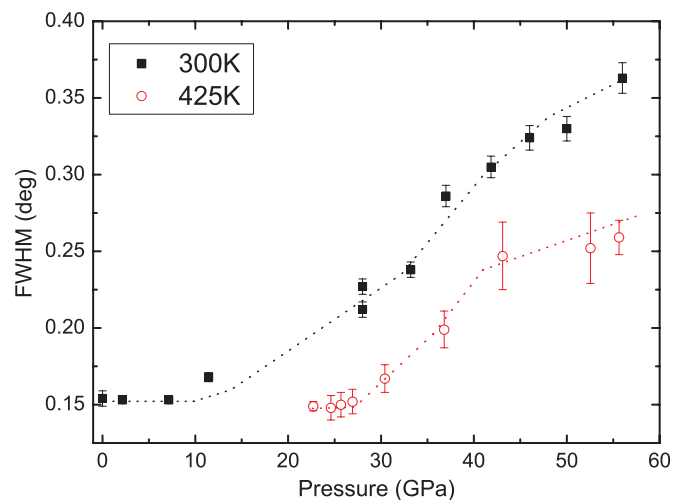


FIG. 2. (Color online) 110 diffraction peak full width at half maximum as a function of pressure as measured under nonhydrostatic conditions. Full squares (black) at ambient temperature, empty circles (red) at 425 K, dotted lines manual fit, guide to the eye.

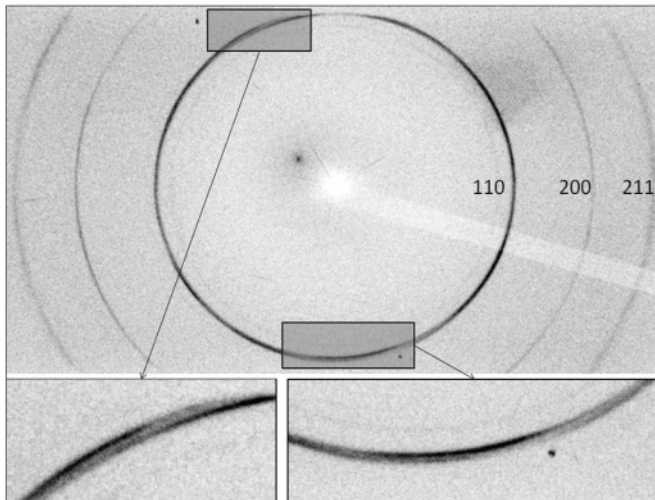


FIG. 3. 2D x-ray diffraction pattern recorded with MAR345 image plate of vanadium compressed under nonhydrostatic conditions at 82 GPa. The rings are indexed corresponding to the low-pressure bcc phase. Magnified inserts at bottom show the splitting of the 110 peak.

entirely analogous to the room temperature experiment. The 110 and 211 bcc diffraction peaks broaden and split while the 200 peak remained as a single sharp peak confirming again the transition from the cubic to rhombohedral phase. The only difference induced by the temperature is a shift of the transition pressure from 30 to $37(\pm 2)$ GPa. This transition pressure is higher than the room temperature value, showing a positive slope for the cubic-rhombohedral vanadium phase boundary on the P-T diagram. The obtained rhombohedral phases for both the 300 and 425 K samples are consistent with previous studies as expected. At the transition pressure of 30 GPa at room temperature we obtain a rhombohedral unit cell with cell parameter $a_R = 2.51031(\pm 0.002)$ Å with $\alpha = 109.61(\pm 0.018)^\circ$, which is smaller than the theoretically expected 110.25° , but consistent with a second-order transition suggested by previous experiments.⁵ A fit of the diffraction pattern to the rhombohedral phase using the JADE software package is shown in Fig. 4. We fit a Vinet-form universal EOS (Ref. 15) to our pressure-volume points for the bcc and rhombohedral phases and obtained the following fitting parameters: $K_0 = 202(\pm 37)$ GPa for the bulk modulus and $K'_0 = 1.71(\pm 1.51)$ for its derivative. These results, with the exception of the bulk modulus derivative, are in good agreement with previous experimental results ($K_0 = 195$ GPa and $K'_0 = 3.5$ (Ref. 5)).

We also performed quasihydrostatic experiments on vanadium samples using different pressure media: Ar, Ne, and He. While Ar is a noble gas it is known that under pressure it stiffens with increasing pressure, becoming a less hydrostatic medium than He or Ne.¹⁶⁻²¹ As expected, we found that the phase transition pressure for vanadium samples in Ar is much closer to the previously reported 63 GPa, which used He as a pressure medium. In our experiments, when vanadium is compressed to 80 GPa in an Ar pressure medium, we found the transition pressure to be 53 GPa. When we change the pressure medium to Ne, which is much softer than Ar at similar pressures, we observed a transition pressure of 61.5 GPa,

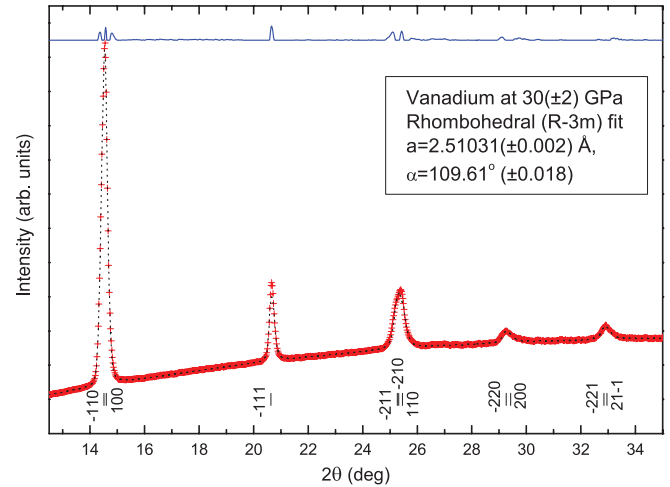


FIG. 4. (Color online) Rietveld refinement of integrated XRD pattern collected from sample compressed without pressure media at $30(\pm 2)$ GPa. Red cross is the experimental data, dashed line is the fit to the rhombohedral structure model, and blue line is the residual to the fit ($\lambda = 0.51822$ Å).

which is very close to the transition pressure of 62 GPa reported by Luo *et al.* as a result of their lattice dynamics calculations and just 1 GPa lower than the experimental data obtained by Ding *et al.* Fitting this data to a Vinet EOS, we find that the vanadium pressure-volume data collected using the Ne pressure medium yields fitting parameters for the bulk modulus and its derivative of $K_0 = 179(8)$ GPa and $K'_0 = 3.11(1.23)$, respectively (see Fig. 5). These parameters are closer to Ding *et al.*'s quasihydrostatic parameters for bcc vanadium and are also in good agreement with the latest theoretical values of $K_0 = 182$ GPa and $K'_0 = 3.75$ published by L. Koči *et al.*²² As anticipated, experiments performed on vanadium in an He pressure medium yielded a transition pressure even higher than the case of the Ne, while the two P-V

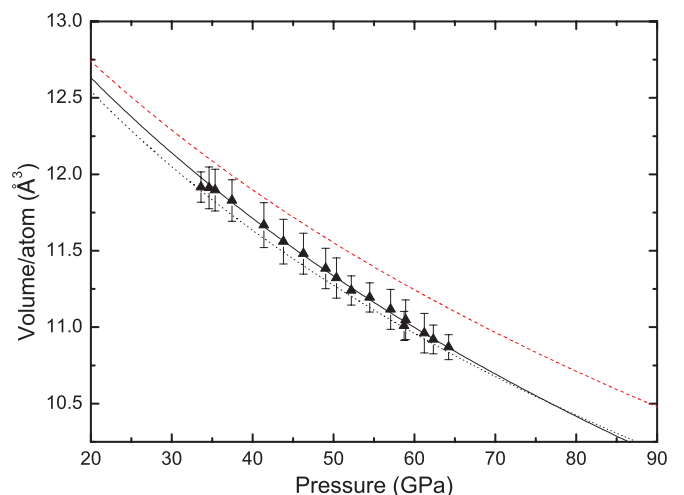


FIG. 5. (Color online) Vanadium unit cell volume as a function of pressure, full triangles, compressed in Ne. Solid black line is the fit to the Vinet EOS with $K_0 = 179(\pm 8)$ GPa and $K'_0 = 3.11(\pm 1.23)$; dashed (red) line is nonhydrostatic, and dotted black line the hydrostatic EOS from Ref. 5.

curves overlapped. We found the transition pressure in the He pressure medium to be 65 GPa, which one can assume to be the lower limit of the transition pressure in an ideal hydrostatic environment. Here we note that regardless of the pressure media used or in experiments without pressure media, to within our experimental errors we do not find a change in unit cell volume across the bcc to rhombohedral transition. The volume change calculated by Lee *et al.* for the first phase transition of 0.03% cannot be experimentally verified since it is within the margin of experimental error.⁷ Based on the contention of Lee *et al.* that the bcc structure of vanadium is mechanically stable, though energetically/thermodynamically unfavorable, in the range where the rhombohedral phase is the ground state,⁷ the transition from bcc to rhombohedral might not occur under all experimental circumstances and the bcc phase may persist as a metastable phase. However, with increasing pressure the metastability may become less energetically stable. Further, nonhydrostatic conditions could provide the mechanical mechanism to overcome any energy barriers to the transition and drive the transition to the rhombohedral phase.

The reported high-pressure rhombohedral phase of vanadium can be characterized as an elongation of the body diagonal of the primitive cell of the bcc unit cell. The strain induced in the sample by the pressure gradients due to nonhydrostatic compression seems to favor deformation along the 111 body diagonal at much lower pressures than in the ideal hydrostatic case. In the ideal situation of hydrostatic conditions at the transition, theoretical calculations reveal that both phases of vanadium are energetically very close to each other and separated by a low-energy barrier that would make it a first-order transition at zero temperature.^{6,7} However, at higher temperatures, because the thermal fluctuations are expected to be larger than the latent heat of the transformation, the true nature of the transition cannot be easily determined. Even if the energy barrier between the bcc and rhombohedral phases is small, it appears that the hydrostaticity of the compression medium directly influences the transition pressure. In the

nonhydrostatic case, when the sample is compressed by the two diamond anvils and contained only by the stiff Re gasket the transition occurs at 30 GPa and as the strength of the pressure media decreases the transition pressure approaches the hydrostatic condition transition pressure. So far there have been no theoretical studies on the influence of the hydrostatic conditions on the transition pressure in vanadium, but in the case of other transition metals the scatter in the transition pressure has been explained by the shear stresses.²³

IV. CONCLUSION

Our experiments confirm the existence of the previously reported rhombohedral phase of vanadium at high pressure. We report a dependence of the transition pressure as a function of the hydrostatic condition of the pressure media. Less hydrostatic conditions lead to a lower transition pressure. We find the bcc→rhombohedral phase transition occurring as low as 30 GPa without any pressure medium and as high as 65 GPa. We propose that the true thermodynamic phase transition pressure should be associated with the 30 GPa value. Higher-pressure transitions are the results of the metastability of the bcc phase due to energy barriers to the transformation. We also report a positive slope for the bcc→rhombohedral transition under nonhydrostatic conditions.

ACKNOWLEDGMENTS

We gratefully acknowledge support from DOE/NNSA Science Campaign-2 and LLNL Science campaign management. This work was performed under the auspices of the US DOE by LLNL under Contract No. DE-AC52-07NA27344. Portions of this work were performed at HPCAT (Sector 16), Advanced Photon Source (APS), Argonne National Laboratory. HPCAT is supported by CIW, CDAC, UNLV, and LLNL through funding from DOE-NNSA, DOE-BES, and NSF. APS is supported by DOE-BES, under Contract No. DE-AC02-06CH11357.

¹J. A. Moriarty, *Phys. Rev. B* **45**, 2004 (1992).

²H. Cynn and C.-S. Yoo, *Phys. Rev. B* **59**, 8526 (1999).

³N. Suzuki and M. Otani, *J. Phys. Condens. Matter* **14**, 10869 (2002).

⁴A. Landa, J. Klepeis, P. Soderlind, I. Naumov, O. Velikokhatnyi, L. Vitos, and A. Ruban, *J. Phys. Condens. Matter* **18**, 5079 (2006).

⁵Y. Ding, R. Ahuja, J. Shu, P. Chow, W. Luo, and H.-K. Mao, *Phys. Rev. Lett.* **98**, 085502 (2007).

⁶B. Lee, R. E. Rudd, J. E. Klepeis, P. Söderlind, and A. Landa, *Phys. Rev. B* **75**, 180101(R), (2007).

⁷B. Lee, R. E. Rudd, J. E. Klepeis, and R. Becker, *Phys. Rev. B* **77**, 134105 (2008).

⁸W. Luo, R. Ahuja, Y. Ding, and H.-K. Mao, *PNAS* **104**, 16428 (2007).

⁹A. Landa, P. Söderlind, A.V. Ruban, O. E. Peil, and L. Vitos, *Phys. Rev. Lett.* **103**, 235501 (2009).

¹⁰Y. Ma, E. Selvi, V. I. Levitas, and J. Hashemi, *J. Phys. Condens. Matter* **18**, S1075 (2006).

¹¹N. Von Barge and R. Boehler, *High Press. Res.* **6**, 133 (1990).

¹²D. Errandonea, Y. Meng, M. Somayazulu, and D. Hausermann, *Physica B* **355**, 116 (2005).

¹³A. P. Hammersley, S. O. Svensson, M. Hanfland, A. N. Fitch, and D. Hausermann, *High. Pres. Res.* **14**, 235 (1996).

¹⁴K. Lagarec and S. Desgreniers, *J. Appl. Crystallogr.* **31**, 109 (1998).

¹⁵P. Vinet, J. Ferrante, J. Rose, and J. Smith, *J. Geophys. Res.* **92**, 9319 (1987).

¹⁶J. H. Burnett, H. M. Cheong, and W. Paul, *Rev. Sci. Instrum* **61**, 3904 (1990).

¹⁷K. Takemura, *J. Appl. Phys.* **89**, 662 (2001).

¹⁸H. Shimizu, H. Imaeda, T. Kume, and S. Sasaki, *Phys. Rev. B* **71**, 014108 (2005).

¹⁹D. Errandonea, R. Boehler, S. Japel, M. Mezouar, and L. R. Benedetti, *Phys. Rev. B* **73**, 092106 (2006).

²⁰A. Dewaele, F. Datchi, P. Loubeyre, and M. Mezouar, *Phys. Rev. B* **77**, 094106 (2008).

²¹S. Klotz, J.-C. Chervin, O. Munsch, and G. Le Marshand, *J. Phys. D: Appl. Phys.* **42**, 075413 (2009).

²²L. Koči, Y. Ma, A. R. Oganov, P. Souvatzis, and R. Ahuja, *Phys. Rev. B* **77**, 214101 (2008).

²³K. J. Caspersen, A. Lew, M. Ortiz, and E. A. Carter, *Phys. Rev. Lett.* **93**, 115501 (2004).